

# ISX9, a small molecule targeting Axin, activates Wnt/ $\beta$ -catenin signaling and promotes hair regrowth

Sapna Sayed<sup>1</sup>, Jiaxing Song<sup>1</sup>, Ling Wang<sup>1</sup>, Boxin Liu<sup>1</sup>, Zijie Su<sup>1</sup>, Li Huan<sup>1</sup>, Vivian Weiwen Xue<sup>1</sup>, Shan-Shan Liu<sup>1</sup>, Xianxiong Chen<sup>1</sup>, Guangqian Zhou<sup>1</sup>, Qi Sun<sup>1</sup>, and Desheng Lu<sup>1</sup>

<sup>1</sup>Shenzhen University

August 23, 2022

## Abstract

**Background and Purpose:** ISX9 is a neurogenesis-promoting small molecule compound which can upregulate the expression of NeuroD1 and induce differentiation of neuronal, cardiac and islet endocrine progenitors. So far, the molecular mechanisms underlying the action of ISX9 still remain elusive. **Experimental Approach:** To identify a novel agonist of the Wnt/ $\beta$ -catenin, a cell-based SuperTOPFlash reporter system was used to screen known-compound libraries. An activation effect of ISX9 on the Wnt/ $\beta$ -catenin pathway was analysed with the SuperTOPFlash or SuperFOPFlash reporter system. Effects of ISX9 on Axin1/LRP6 interaction were examined using a mammalian two-hybrid system, co-immunoprecipitation, microscale thermophoresis (MST), emission spectra and mass spectroscopy assays. The expression of Wnt target and stemness marker genes were evaluated with real-time PCR and immunoblotting. In vivo hair regeneration abilities of ISX9 were analysed by immunohistochemical staining, real-time PCR and immunoblotting in hair regrowth model using C57BL/6J mice. **Key Results:** In this study, ISX9 was identified as a novel agonist of the Wnt/ $\beta$ -catenin pathway. ISX9 targeted Axin1 by covalently binding to its N-terminal region and potentiated the LRP6-Axin1 interaction, thereby resulting in the stabilization of  $\beta$ -catenin and upregulation of Wnt target genes and stemness marker genes. Moreover, the topical application of ISX9 markedly promoted hair regrowth in C57BL/6J mice and induced hair follicle transition from telogen to anagen via enhancing Wnt/ $\beta$ -catenin pathway. **Conclusions and Implications:** Taken together, our study unraveled that ISX9 could activate Wnt/ $\beta$ -catenin signaling by potentiating the association between LRP6 and Axin1, and may be a promising therapeutic agent for alopecia treatment

**ISX9, α σμαλλ μολεκυλε ταργετινγ Αξιν, αστιατες Ωντ/β-σατενιν σιγναλινγ ανδ προ-μοτες ηαιρ ρεγρωτη**

**Running Title:** ISX9 activates Wnt/ $\beta$ -catenin Signaling

Sapna Sayed<sup>1</sup>, Jiaxing Song<sup>1, 2</sup>, Ling Wang<sup>1</sup>, Boxin Liu<sup>1</sup>, Zijie Su<sup>1</sup>, Huan Li<sup>1</sup>, Vivian Weiwen Xue<sup>1</sup>, Shanshan Liu<sup>1</sup>, Xianxiong Chen<sup>3</sup>, Guangqian Zhou<sup>3</sup>, Qi Sun<sup>1\*</sup> and Desheng Lu<sup>1\*</sup>

<sup>1</sup> Guangdong Provincial Key Laboratory of Regional Immunity and Diseases, International Cancer Center, Department of Pharmacology, Shenzhen University Health Science Center, Shenzhen, China

<sup>2</sup> Medical Scientific Research Center, Life Sciences Institute, Guangxi Medical University, Nanning, China

<sup>3</sup> Department of Physiology, School of Medicine, Health Science Center, Shenzhen University, Shenzhen, China

\* To whom correspondence may be addressed. Qi Sun or Desheng Lu, Shenzhen University Health Science Center, Shenzhen 518060, Guangdong, China.

Email: sunqi@szu.edu.cn or delu@szu.edu.cn.

**DATA AVAILABILITY STATEMENT**

The data that support the findings of this study are available from the corresponding authors upon reasonable request.

Words Count (Excluding Abstract/ Methods/References/Figure Legends): 3396

## ACKNOWLEDGEMENTS

We would like to acknowledge the support provided by International Science and Technology Cooperation: Carson Cancer Stem Cell Vaccines R&D Center, Shenzhen University. This work was supported by the National Natural Science Foundation of China (31970739, 81802662, 31900881, and U21A20421), the Natural Science Foundation of Guangdong Province (2020A1515010340, 2020A1515010543 and 2022A1515010598), the Shenzhen Key Basic Research Program (JCYJ20200109105001821), the Shenzhen Natural Science Fund (the Stable Support Plan Program) (20200826134656001).

## DECLARATION OF CONFLICT OF INTERESTS

The authors declare no competing interests.

## AUTHORS CONTRIBUTIONS

D L designed the research; S S, J S, L W, B L, Z S, H L, V W X, S L, X C and Q S performed experiments; S S, G Z, Q S, and D L carried out the data analysis. D L, L W, S S, Q S, and G Z made critical comments on the manuscript. S S, Q S and D L wrote and edited the manuscript.

## ABSTRACT

### Background and Purpose:

ISX9 is a neurogenesis-promoting small molecule compound which can upregulate the expression of NeuroD1 and induce differentiation of neuronal, cardiac and islet endocrine progenitors. So far, the molecular mechanisms underlying the action of ISX9 still remain elusive.

**Experimental Approach:** To identify a novel agonist of the Wnt/ $\beta$ -catenin, a cell-based SuperTOPFlash reporter system was used to screen known-compound libraries. An activation effect of ISX9 on the Wnt/ $\beta$ -catenin pathway was analysed with the SuperTOPFlash or SuperFOPFlash reporter system. Effects of ISX9 on Axin1/LRP6 interaction were examined using a mammalian two-hybrid system, co-immunoprecipitation, microscale thermophoresis (MST), emission spectra and mass spectrometry (MS) assays. The expression of Wnt target and stemness marker genes were evaluated with real-time PCR and immunoblotting. *In vivo* hair regeneration abilities of ISX9 were analysed by immunohistochemical staining, real-time PCR and immunoblotting in hair regrowth model using C57BL/6J mice.

**Key Results:** In this study, ISX9 was identified as a novel agonist of the Wnt/ $\beta$ -catenin pathway. ISX9 targeted Axin1 by covalently binding to its N-terminal region and potentiated the LRP6-Axin1 interaction, thereby resulting in the stabilization of  $\beta$ -catenin and upregulation of Wnt target genes and stemness marker genes. Moreover, the topical application of ISX9 markedly promoted hair regrowth in C57BL/6J mice and induced hair follicle transition from telogen to anagen via enhancing Wnt/ $\beta$ -catenin pathway.

**Conclusions and Implications:** Taken together, our study unraveled that ISX9 could activate Wnt/ $\beta$ -catenin signaling by potentiating the association between LRP6 and Axin1, and may be a promising therapeutic agent for alopecia treatment.

**Key words:** ISX9, Wnt/ $\beta$ -catenin signaling, LRP6/Axin1 interaction, alopecia

### Bullet point summary

#### What is already known

- ISX9 has been identified as a neurogenesis inducer
- ISX9 could induce differentiation of neuronal, cardiac and islet endocrine progenitors. **What this study adds**

- ISX9 is a novel activator of Wnt/ $\beta$ -catenin signaling and targets Axin1 via its N-terminal region.
- ISX9 potentiates the LRP6-Axin1 association and thereby, resulting in stabilization of  $\beta$ -catenin. **What is the clinical significance**
- ISX9 may be a promising therapeutic agent for alopecia treatment via upregulating Wnt/ $\beta$ -catenin signaling

## 1 INTRODUCTION

Hair loss or alopecia is a highly prevalent dermatological disorder which can impair the quality of life and cause a lifetime of mental suffering. Hair loss is influenced by multiple factors such as genetic factors, hormonal dysfunction, sebum content, aging, mental disorders and environmental factors (Jang et al., 2013; Patel, Harrison, & Sinclair, 2013; Pratt, King, Messenger, Christiano, & Sundberg, 2017). Despite enormous effort in developing drugs to treat alopecia, only minoxidil and finasteride have been approved by the US Food and Drug Administration (FDA) for clinical practice (Libecco & Bergfeld, 2004; Linas & Nies, 1981; Van Neste et al., 2000). Minoxidil is an antihypertensive vasodilator (Sica, 2004). Finasteride can block the conversion of testosterone to dihydrotestosterone and is used to treat alopecia patients unresponsive to minoxidil (Bolduc & Shapiro, 2000). Both drugs have limited efficacy in alopecia treatment and possess significant adverse effects. The effect of both drugs is not long lasting and require prolonged use. Patients using finasteride may have serious side effects on sexual and reproductive health. Minoxidil can produce pruritus, irritant dermatitis, and dizziness during treatment. Therefore, there is an urgent need to develop drugs with novel mechanisms of action for the treatment of alopecia.

The Wnt/ $\beta$ -catenin signaling pathway plays a crucial role in hair morphogenesis, hair growth, hair cycling and regeneration (Andl, Reddy, Gaddapara, & Millar, 2002; Oujii et al., 2008; Zhou et al., 2016). The substantial stabilization of the free  $\beta$ -catenin is indispensable for the Wnt/ $\beta$ -catenin pathway, which is controlled by a destruction complex. In this destruction complex, the scaffolding protein Axin interacts and takes into proximity to the other components comprising the adenomatous polyposis coli protein (APC), the casein kinase 1 (CK1) and the glycogen synthetase kinase  $3\beta$  enzyme (GSK $3\beta$ ). The  $\beta$ -catenin protein is phosphorylated by GSK $3\beta$ , resulting in its ubiquitination-mediated degradation. The Wnt/ $\beta$ -catenin pathway is triggered when the Wnt proteins bind to their receptors Frizzled (Fzd) and low-density lipoprotein receptor-related proteins 5/6 (LRP5/6). A critical step in Wnt pathway stimulation is the recruitment of the Axin complex towards the LRP5/6 receptor complex (Clevers & Nusse, 2012). The Axin complex peculiarly interacts with LRP5/6 cytoplasmic tail, facilitating the phosphorylation of LRP5/6, which hinders  $\beta$ -catenin phosphorylation and constitutive degradation (Tamai et al., 2000; Zeng et al., 2005). Consequently, the stabilized  $\beta$ -catenin hoards in the cytoplasm and is translocated into the nucleus, where it binds with the T-cell factor/lymphoid enhancer factor 1 (TCF/LEF1) transcription factors to trigger the expression of Wnt signaling target genes, including Axin2, LEF1, Fibronectin and Survivin (Nusse & Clevers, 2017).

Previous studies found that nuclear  $\beta$ -catenin existed in chick feather prior to placode formation, and LEF1 highly expressed in mouse dermis during vibrissa follicle formation, indicating the involvement of Wnt/ $\beta$ -catenin signaling in follicular development (Kratochwil, Dull, Farinas, Galceran, & Grosschedl, 1996; Noramly, Freeman, & Morgan, 1999). Subsequent studies further revealed that multiple Wnt molecules could stimulate hair follicle stem cells and promote hair regeneration via activating  $\beta$ -catenin signaling (Hu et al., 2021). Dong et al demonstrated that treatment with Wnt1a-enriched conditioned media could accelerate the progression of hair follicle from telogen to anagen, upregulate the expression of hair induction-associated genes, and enhance the amount of hair in depilated mouse skin (Dong et al., 2014). Wnt10b has been shown to increase the growth of hair follicle by enhancing telogen to anagen switch via  $\beta$ -catenin stabilization (Wu, Zhu, Liu, Liu, & Li, 2020). Wnt3a has been found to activate  $\beta$ -catenin signaling and promote hair growth in nude mice receiving skin reconstitution (Xing, Yi, Miao, Su, & Lei, 2018). Rajendran et al reported that treatment with Wnt3a and Wnt7b-enriched macrophage-extracellular vesicle significantly increased the proliferation and migration of dermal papilla cells via enhancing the Wnt/ $\beta$ -catenin pathway (Rajendran et al., 2020). In contrast, the Wnt signaling antagonist DKK1 could trigger anagen-to-catagen transition when injected into the hypodermis of C57BL/6 mice, while neutralizing DKK-1 antibody delayed catagen

progression in mice (Kwack, Kim, Kim, & Sung, 2012). Overall, these studies highlight the Wnt/ $\beta$ -catenin signaling pathway as a promising therapeutic target for hair loss.

The small molecule isoxazole-9 [ISX9, N-cyclopropyl-5-(thiophen-2-yl)isoxazole-3-carboxamide] has been identified as a neurogenesis inducer through high-throughput screening of chemical libraries in stem cell-based assays (Schneider et al., 2008). ISX9 was found to potentiate cell proliferation and increase the number or differentiation of neurons in the hippocampal dentate gyrus in a myocyte-enhancer factor 2 (MEF2)-dependent manner (Bettio et al., 2016). ISX9 could also induce intracellular  $\text{Ca}^{2+}$  influx which activates phosphorylated CaMK and regulates nuclear export of the MEF2 modulator HDAC5, thus allowing neuronal differentiation (Koh et al., 2015). In other tissues, ISX9 was shown to induce differentiation of cardiac and islet endocrine progenitors (Tsakmaki, Fonseca Pedro, Pavlidis, Hayee, & Bewick, 2020; Xuan et al., 2018). Dioum et al demonstrated that ISX9 increased the expression and secretion of insulin in islets and upregulated the expression of neuronal differentiation 1 (NeuroD1) and other regulators of islet differentiation (Dioum et al., 2011). Kalwat et al also reported that ISX9 could alter  $\beta$ -cell metabolites, protect glucose-responsive signaling pathways under lipotoxic conditions, and improve glycemia in a mouse model of  $\beta$ -cell regeneration (Kalwat et al., 2016). However, the molecular mechanism of ISX9 action remains unclear. In the present study, ISX9 was identified as a novel activator of the Wnt/ $\beta$ -catenin signaling pathway. We further investigated the mechanism involved in activation of Wnt/ $\beta$ -catenin signaling by ISX9. Finally, our results demonstrated that ISX9 could stimulate the proliferation of hair follicle and promote hair growth in mice through activating the Wnt signaling pathway.

## 2 METHODS

### 2.1 Cell culture

The human embryonic kidney 293T (HEK293T) cells (ATCC Cat#CRL-3216; RRID: CVCL-0063), the human keratinocyte (HaCaT) cells (ATCC Cat#CRL-2309; RRID: CVCL-0038), and the mouse embryonic fibroblasts (NIH3T3) cells (ATCC Cat# CRL-1658, RRID:CVCL\_0594) were acquired from American Type Culture Collection (ATCC, Manassas, VA, USA) and sustained in Dulbecco's Modified Eagle's Medium (DMEM) (Thermo Fisher Scientific, Cat#C11995500BT, Waltham, MA, USA) accompanied with 10% fetal bovine serum (FBS) (Thermo Fisher Scientific, Cat# 10270-106, Shanghai, China). Cells were cultured with 120  $\mu\text{g}/\text{mL}$  penicillin along with 200  $\mu\text{g}/\text{mL}$  streptomycin (Thermo Fisher Scientific, Cat# 15-140-122, Shanghai, China) at 37 °C in an incubator with 5%  $\text{CO}_2$ . ISX9 was dissolved in dimethyl sulfoxide (DMSO) for provision of a stock solution at a final concentration of 20 mM. For treating cells, 20 mM stock solution was diluted with the specific media with respect to cells, and the final DMSO concentration was <0.1%.

### 2.2 Plasmids and screening of drug library

Following the manufacturer's instruction, the transfection of HEK293T and HaCat cells were performed using Lipofectamine 2000 transfection reagent (Roche Diagnostics GmbH, Cat#11668-019, Mannheim, Germany). The reporter plasmids SuperTOPFlash was modestly gift of Karl Willert (University of California, San Diego, CA, USA) while SuperFOPFlash was bought from Beyotime (Beyotime Biotechnology, Cat# D2503, Shenzhen, China). For the construction of C-terminally V5-tagged LRP6 expression plasmid, the cDNA encoding LRP6 was amplified by RT-PCR and cloned into the pcDNA 3.1/V5-His mammalian expression vector. The N-terminally tagged Flag-Axin1 expression plasmid was built by inserting the conforming cDNA into the pFlag-CMV2 expression vector.

For drugs screening, HEK293T cells were fully-fledged in 10 cm plates. After 24 h, achieving 50% convergence, cells were transfected with 5  $\mu\text{g}$  of SuperTOPFlash or SuperFOPFlash reporters, hauler DNA pcDNA3 and 1  $\mu\text{g}$  of control-plasmid pCMX- $\beta$ -gal ( $\beta$ -galactosidase,  $\beta$ -gal) amassing a total of 10  $\mu\text{g}/\text{plate}$ . After 24 h-transfection, cells were placid and disseminated in 96-well microtiter plates. Finally, cells were treated with different drugs for the preliminary screen. Exploiting a microtiter plate luminometer, the 24 h-incubated cells were lysed and activities of luciferase were detected using a luciferase assay kit (Promega Cat# E1501, Madison, WI, USA). Making use of the  $\beta$ -galactosidase as an internal control, the values from luciferase assay were normalized for distinctions in transfection efficiency.

## 2.3 Protein purification

The expression plasmids for His-tagged intracellular domain of LRP6/1394-1613 (His-LRP6-ICD), GST-tagged Axin1 1-300 (GST-Axin1-300), GST-tagged Axin1 301-521 (GST-Axin301-521), and GST-tagged Axin1 522-862 (GST-Axin522-862) were constructed and expressed in *Escherichia coli* (*E. coli*) BL21. The expression of fusion proteins was induced with IPTG (Sigma-Aldrich, Shanghai, China) at 16 or 28 °C for 8-12 h. His-LRP6-ICD was purified by NiNTA Purification System, while GST and GST fusion proteins were purified by affinity chromatography with glutathione-sepharose 4B beads (GE Healthcare, Piscataway, NJ, USA). The factor Xa protease was used to remove GST and His tag from fusion proteins.

## 2.4 RNA extraction and real-time PCR analyses

Following manufacturing's guideline, RNA was extracted employing RNAsiso Plus (TaKaRa Cat# 9109, Kusatsu, Shiga, Japan). The isolated total RNA is then converted into cDNA by means of the Primescript RT Reagent Kit (TaKaRa Cat# RR037A, Kusatsu, Shiga, Japan) following the manufacturer's practice. The cDNA was next utilized for quantitative PCR analysis by an ABI Prism 7300 Real-Time PCR System (Applied Biosystems, Foster City, CA, USA) via qPCR Master Mix (Bimake Cat# B21203, Houston, TX, USA). Quantification of mRNA levels of human and mouse genes i.e., Axin2, LEF1, Fibronectin, Survivin, OCT4, Twist1, LGR5, and SOX2 were carried out. The "comparative Ct method" was accomplished to evaluate relative countenance of genes. The data are obtained as the fold change. The fold change was premeditated as  $2^{-\Delta\Delta Ct}$  ( $\Delta\Delta Ct = \Delta Ct_{treated} - \Delta Ct_{control}$ , Ct is the cycle figure at spot where fluorescence first surpasses the threshold). The  $\Delta Ct$  values from each target gene were obtained by subtracting the values for GAPDH Ct from the illustration Ct. The data of three technical replicates/sample are presented. The primer sequences are shown in supplementary tables (Supplementary Table S1 and S2).

## 2.5 Immunoblot Analysis

For extraction of proteins, cells or mice-skin tissues were treated with RIPA buffer (20 mM Tris-HCl -pH 7.4, 150 mM NaCl, 1 % Triton X-100, 0.1 mM DTT, 1 mM EDTA, 1 mM EGTA, and 1 mM PMSF) containing the protease and phosphatase inhibitor cocktail (Topscience) trailed by sonication. The protein extraction was then fractionated by SDS-PAGE and passed-on to PVDF membranes (Cat# ISEQ00005, Millipore, Burlington, MA, USA). Western blotting was accomplished with the subsequent primary antibodies: anti- $\beta$ -catenin (1:2,000, Santa Cruz Biotechnology Cat# sc-7963, RRID:AB\_626807), anti-LGR5 (1:1,000, Abcam Cat# ab75732, RRID:AB\_1310281), anti-SOX2 (1:1,000, Cell Signaling Technology Cat# 23064, RRID:AB\_2714146), anti-Flag (1:5,000, Sigma-Aldrich Cat# F1804, RRID:AB\_262044), anti-GAPDH (1:5,000, Transgen Biotech Cat# HC301-02, RRID:AB\_2629434), anti-LRP6 antibody (1:1000 Cell Signaling Technology Cat# 2560, RRID:AB\_2139329), anti-CK1 $\epsilon$  antibody (1:1000 Cell Signaling Technology Cat# 12448, RRID:AB\_2797919), anti-active  $\beta$ -catenin antibody (1:1000 Cell Signaling Technology Cat#8814, RRID:AB\_11127203), anti-LEF1 antibody (1:1000 Cell Signaling Technology Cat#76010, RRID:AB\_2799877), anti-Axin2 antibody (1:1000 Cell Signaling Technology Cat# 2151, RRID:AB\_2062432), anti-V5 antibody (1:1000 Cell Signaling Technology Cat#13202, RRID:AB\_2687461), anti-Survivin antibody (1:1000 Santa Cruz Biotechnology Cat# sc-17779, RRID:AB\_628302), anti-pLRP6 antibody (1:1000 Cell Signaling Technology Cat# 2568 RRID:AB\_2139327), anti-GSK-3-beta (1:1000 Cell Signaling Technology Cat#9315S RRID:AB\_490890), anti-Twist1 (1:1000 Cell Signaling Technology Cat#46702S RRID:AB\_2799308), anti-Phospho-GSK-3 $\beta$  (1:1000 Cell Signaling Technology Cat#9322S RRID:AB\_2115196), and Anti cytokeratin 17 (1:1000, Abcam Cat# ab53707, RRID:AB\_869865). Western blotting was carried out with the chosen primary antibodies with nurture of 4 °C overnight. Next, the PVDF membranes were mounting with HRP (Horse-radish Peroxidase) conjugated goat anti-rabbit (1:10,000, Thermo Fisher Scientific Cat# A16096, RRID:AB\_2534770) or anti-mouse (1:10,000, Thermo Fisher Scientific Cat# A16066, RRID:AB\_2534739) or IgG at room temperature for 1 h. After incubating with substrate of ECL Plus-Western-Blotting (Thermo Fisher Scientific, Cat# 32132), the immunoblots were established by Chemiluminescent Imaging System (Tanon 5200, Shanghai, China).

## 2.6 Co-immunoprecipitation assays

HEK293T and HaCaT cells ( $0.5 \times 10^6$  cells per well) were scattered in six-well plates, and treated with the indicated concentrations of ISX9 or DMSO for 24 h. The pooled of 100  $\mu\text{g}$  protein-lysates were accrued by using 500  $\mu\text{L}$  RIPA initially (phosphatase inhibitor cocktails and protease inhibitor freshly added), after that centrifugation is executed (12,000 rpm for 15 min at 4 °C). After quantification, the lysates were established with respective antibodies at 4 °C overnight. By using anti-Flag agarose bead (Bimake), we then enacted an immunoprecipitation. The immunocomplexes were washed five times with RIPA buffer and boiled in the SDS-loading buffer. They were then resolute by 10% SDS-PAGE and relocated to PVDF membranes, stalked by immunoblotting with the stipulated antibodies.

## 2.7 Microscale thermophoresis

Microscale thermophoresis (MST) experiments were conducted on a Monolith NT.115 system (NanoTemper Technologies GmbH, Germany), which was used to quantify the interaction between Axin1 fragments (Axin1 1-300, Axin1 301-521, Axin1 522-862) and ISX9, and the interaction between LRP6-ICD and ISX9, respectively. Axin1 fragments or LRP6-ICD were labeled with the manufacturer's labeling kits (Monolith<sup>TM</sup> RED-NHS, NanoTemper Technologies GmbH, Germany). During the measurement of Axin1 fragments with ISX9, the concentration of labeled Axin1 fragments or LRP6-ICD is 100 nM. Unlabeled ISX9 was prepared in 10 mM PBS dimethyl sulfoxide (DMSO), with the final concentrations of ISX9 ranging from 0.61 nM to 5  $\mu\text{M}$ , the samples were added to the monolith capillaries (MO L022, NanoTemper Technologies) and subsequently subjected to MST analysis. The values obtained were normalized and plotted against the Axin1 fragments or LRP6-ICD and ISX9 concentration, respectively. The dissociation constant was then determined using a single-site model to fit the curve.

## 2.8 Emission spectra

Axin1 protein fragment was titrated into ISX9, and the mixtures were allowed to equilibrate at room temperature for 2 min. Emission spectra were recorded in the 520-680 nM range using an excitation wavelength of 465 nM. The change of luminescence intensity was observed by a fluorescence spectrometer (Edinburgh FS5, UK).

## 2.9 Mass spectrometry assays

10  $\mu\text{L}$  ISX9 at 1 mM in PBS was incubated with 40  $\mu\text{L}$  purified flag-tagged Axin1 1-300 (1 mg/mL) overnight at 4 °C. All analyses were performed using a Thermo Scientific Ultimate 3000 Binary UHPLC system (Thermo Fisher Scientific, Germering, Germany) coupled online to a Thermo Scientific Ultra High Mass Range Q Exactive hybrid quadrupole-Orbitrap mass spectrometer using an IonMax API source with a HESI-II probe (Thermo Fisher Scientific, Bremen, Germany).

The separation of protein-ligand in ACQUITY UPLC Protein BEH C4 (300A, 21 mm $\times$ 150 mm, 1.7  $\mu\text{m}$ ) was performed by using 0.1% TFA water and 0.1% TFA in ACN as mobile phases A and B, respectively. A gradient of 20% to 60% B in 8 min, followed by 60% to 80% B in 0.1 min was applied. Following the analytical gradient, an isocratic step at 80% B for 3 min was used to wash the column, followed by 4 min of column re-equilibration at 20% B. The flow rate was 0.2 mL/min, column temperature 60 °C and injection volume 4  $\mu\text{L}$  (1 mg/mL sample material). The UV acquisition wavelength was 214 nm.

Full MS spectra were acquired in positive polarity in a scan range of 500–4,000 m/z. The resolution was set to 17,500 at 400 m/z, with an AGC target of 3e6 ions and 5 microscans were performed. The maximum injection time was 200 ms. In-source trapping desolvation was set to 20 V, and the trapping gas pressure was set to 7.0. Sheath gas was set to 35 arbitrary units (AU) and auxiliary gas was set to 10 AU. The spray voltage was 3.8 kV, the capillary temperature was 300 °C, the S-lens RF was set to 80 V and the auxiliary gas heater temperature was 300 °C.

Mass spectra were acquired using Thermo Scientific Xcalibur version 4.1.31.9. The analysis of the acquired mass spectra was carried out using the Thermo Scientific BioPharma Finder software version 3.1.

## 2.10 Animal model studies

All animal care and experimental techniques for anesthetics, hair regrowth experiments and assays were accomplished with the permission of Animal Research Ethics Committee of Shenzhen University (permit number AEWC-201412003). Animal studies are stated in amenability with the ARRIVE guidelines and with the commendations made by the British Journal of Pharmacology (Lilley et al., 2020) Specific pathogen-free C57BL/6 mice (6 weeks old) were purchased from Nanjing Biomedical Research Institute of Nanjing University, (Nanjing, China) and acclimatized for 1 week. After anesthesia via an intraperitoneal injection of 2,2,2-tribromoethanol (Sigma-Aldrich, St. Louis, USA), the skin hairs on the dorsal side of 7-week-old mice (whose hair follicles were in the telogen phase) were clean-shaven by a hair clipper. The mice were randomly separated into three groups(Lee et al., 2012).. For every mouse, 200  $\mu$ L of each drug was topically applied at an appropriate concentration everyday (as described in figure legends) for 25 days. The control group received vehicle alone, the ISX9 group received vehicle containing 1% of ISX9, and the minoxidil group received 2% of minoxidil. All reagents used for the hair growth test were dissolved in a vehicle composed of 50% (v/v) ethanol, 30% water, and 20% propylene glycol. The back skin of the mice was photographed at 0, 7, 14, 21, 25 days, and analyses was done regarding the weight of regrown hair in different groups treated for 25 days. After killing mice, skin tissues were gathered and saved at -80 °C.

### 2.11 Histology and immunohistochemistry analyses

Samples were immobile in 4% formaldehyde in PBS for 24 h, then dehydrated and implanted in paraffin, sectioned at 5  $\mu$ m before haematoxylin and eosin (H&E) staining and immunohistochemistry were accomplished. The primary antibodies exploited for immunohistochemistry include anti-Ki-67 (1:200, Cell Signaling Technology Cat# 12202, RRID:AB\_2620142), anti-LGR5 (1:100, Abcam Cat# ab75732, RRID:AB\_1310281), Anti-active  $\beta$ -catenin antibody (1:100 Cell Signaling Technology Cat#8814, RRID:AB\_11127203) and anti- $\beta$ -catenin (1:100 Cell Signaling Technology Cat# 9562, RRID:AB\_331149).

### 2.12 Hair cycle analyses

The analyses of hair cycle were centered on level of skin pigmentation and hair shaft growth, as earlier reported (Stenn & Paus, 2001). Briefly, clean-shaved hair-coat-recovery values were premeditated based on skin pigmentation levels from 0 to 100% (Chai et al., 2019). For illustration, 0% implied no hair growth (and no pigmentation); 50% couched full-length just grown hairs casing half of the dorsal designated skin (or pigmentation level on 100% of the dorsal definite skin area without any hair shafts); 70% implicit full-length-hair progress on  $\sim$ 70% of the dorsal skin (or pigmentation level covering 100% of dorsal skin along with 30–40% hair shafts); 100% inferred afresh full-length hair growth.

### 2.13 Hair follicles count

The H&E stained slides were photographed using a digital photomicrograph and all of the images were cropped in a fixed width of 300 pixels. We counted hair follicles manually in a fixed area (0.09 mm<sup>2</sup>). Digital photomicrographs were taken from representative areas at a fixed magnification of 100X.

### 2.14 Data and statistical analyses

All experiments were equal sized, randomized and blinded. No data values were omitted in any statistical analysis. The data and statistical analysis according to the recommendations of the *British Journal of Pharmacology* on experimental design and analysis in pharmacology (Curtis et al., 2018). Statistical analyses were acquired with GraphPad prism7.00 software (GraphPad, RRID: SCR\_000306). The data were evaluated by Student's t test or one- way ANOVA followed by Dunnett's t test. Results are presented as mean  $\pm$  SD. Differences at P < 0.05, were considered statistically significant.

### 2.15 Materials

ISX9 was obtained from TargetMol (Cat#T2003 CAS 832115625, Shanghai, China). Minoxidil was also purchased from TargetMol (Shanghai, China). Reagents for cell culture were bought from GIBCO. Compound libraries consist of antifungal, antibacterial and antiviral agents, were acquired from MedChemExpress (MCE,

Monmouth Junction, NJ, USA). All additional chemical reagents were attained from Sigma-Aldrich (St. Louis, MO, USA) apart from reagents with special instructions.

### 3 RESULTS

#### 3.1 ΙΣΞ9 αστιατες της Ωντ/β-κατενιν σιγναλιγ πατηωαψ

In order to identify novel small molecules that modulate the Wnt/ $\beta$ -catenin signaling pathway, a cell-based SuperTOPFlash reporter system was used to screen a known-compound library. Our screening identified ISX9, a small molecule with the isoxazole scaffold, as a potential activator of Wnt/ $\beta$ -catenin signaling (Figure 1A and B). To determine the agonistic effect on the Wnt/ $\beta$ -catenin pathway, the luciferase reporter SuperTOPFlash was transfected into HEK293T cells. Treatment with 2.5-40  $\mu$ M ISX9 strongly increased the transcriptional activity of the SuperTOPFlash reporter in a dose-dependent manner. ISX9 at 40  $\mu$ M could induce the reporter activity  $\sim$ 2700-fold above the basic levels (Figure 1C). However, ISX9 had little effect on the activity of negative control reporter SuperFOPFlash, which contains mutated TCF-binding elements. As anticipated, lithium chloride (LiCl), a well-known activator of Wnt signaling, remarkably increased the activity of the SuperTOPFlash reporter (Figure 1D).

To further confirm the effect of ISX9 on Wnt signaling, we performed the SuperTOPFlash reporter assay in human keratinocyte HaCaT cells. Similarly, ISX9 dose-dependently enhanced the activity of the SuperTOPFlash reporter in HaCat, while it did not affect the SuperFOPFlash reporter activity (Figure 1E). Together, these results demonstrated that ISX9 is capable of activating the Wnt/ $\beta$ -catenin pathway.

#### 3.2 ΙΣΞ9 ινδυσες της αςσυμυλατιον οφ β-κατενιν ιωιτηουτ αφρεστινγ της εξπρεσσιον ανδ αςτιιτψ οφ ΛΡΠ6 ανδ ΓΣΚ3β

To explore the potential target of ISX9 action in the Wnt signaling cascade, we examine the effect of ISX9 on key components in Wnt signaling cascade, including active  $\beta$ -catenin, total  $\beta$ -catenin, phosphorylated LRP6, total LRP6, Ser9 phosphorylated GSK3 $\beta$ , total GSK3 $\beta$ , and CK1e in HEK293T, HaCat and NIH3T3 cells. As shown in Figure 2, ISX9 treatment dramatically upregulated protein levels of active  $\beta$ -catenin and total  $\beta$ -catenin in a concentration-dependent fashion, whereas it had little effect on the levels of phosphorylated LRP6, total LRP6, Ser9 phosphorylated GSK3 $\beta$ , total GSK3 $\beta$ , and CK1e in all three cell lines. We also checked ISX9 effect on mRNA expression of  $\beta$ -catenin in HEK293T cells. There was no significant change in mRNA expression of  $\beta$ -catenin in response to ISX9 treatment (Supplementary Figure S1). Collectively, these results imply that ISX9 could activate Wnt/ $\beta$ -catenin signaling mainly through inducing the accumulation of intracellular  $\beta$ -catenin without affecting the expression and activity of LRP6 and GSK3 $\beta$ .

#### 3.3 ISX9 potentiates the association of LRP6 with Axin1

It has been known that Wnt stimulation-induced LRP6 phosphorylation promotes the association of LRP6 with Axin, a key step to regulate  $\beta$ -catenin stability (Xin Zeng et al., 2008). We therefore examined the effect of ISX9 on interaction between LRP6 and Axin1 using a mammalian two-hybrid assay consisted of UAS-TK-Luc reporter and the expression vectors for Gal4-LRP6 intracellular domain (Gal4-LRP6-ICD) and VP16-Axin1. The interaction between LRP6-ICD and Axin1 was observed in HEK293T cells transfected with both Gal4-LRP6-ICD and VP16-Axin1, and treatment with ISX9 dose-dependently potentiated the interaction between LRP6-ICD and Axin1. However, little signal was detected when UAS-TK-Luc reporter was co-expressed with either Gal4-LRP6-ICD or VP16-Axin in the presence or absence of ISX9 (Figure 3A). Notably, LiCl treatment exerted little effect on the association of Gal4-LRP6 ICD with VP16-Axin1 (Figure 3B). These results suggest that ISX9 may potentiate the association of LRP6 with Axin1. To further confirm the effect of ISX9 on the interaction of LRP6 with Axin1, a co-immunoprecipitation assay was performed using anti-Flag beads in HEK293T cells transfected with LRP6-V5 and Flag-Axin1 expression vectors. Figure 3C showed that increasing amounts of LRP6-V5 protein were immunoprecipitated using anti-Flag beads in the presence of ISX9 (Figure 3C). Treatment with ISX9 also promoted endogenous interaction between LRP6 and Axin1 in HEK293T and HaCat cells (Figure 3D and E). These results demonstrated that ISX9 is capable of promoting the interaction of LRP6 with Axin1.

### 3.4 ISX9 enhances the interaction of LRP6-ICD with Axin1 through covalently binding to the N-terminal region of Axin

To explore the mechanism through which ISX9 potentiates the protein-protein interaction between LRP6 and Axin1, a microscale thermophoresis (MST) analysis was performed to determine whether ISX9 could directly bind to LRP6 and Axin1. We expressed and purified the three truncated forms of Axin1, Axin1-300 (aa 1–300), Axin301-521 (aa 301-521) and Axin522-862 (aa 522-862), and LRP6-ICD domain as His-tagged fusion proteins. The results showed the titration of ISX9 to fluorescently labeled Axin1-300, yielded dose-dependent upward-shifted thermophoresis profiles with a Kd value of 595 nM (Figure 4A), suggesting the direct binding between ISX9 and Axin1-300. However, no detectable binding was observed between ISX9 and Axin301-521 (Figure 4B), Axin522-862 (Figure 4C) or LRP6-ICD (Figure 4D). The fluorescence emission spectra also showed that ISX9 could interact with purified Axin1-300 protein (Figure 4E).

Next, mass spectrometry was used to verify ISX9 binding mode with Axin1-300. The molecular weight of recombinant Axin1-300 is about 31417.38 Da. We detected an extra peak at 31650.81 Da after incubating purified Axin1-300 fragment with ISX9 (233.44 Da) (Figure 4F), indicating that covalent binding was formed between ISX9 and Axin1-300.

### 3.5 ISX9 ινιβιτις τικε ασσοκιατιον οφ Αξιν1 ιικη β-κιατενιν

Axin is a vital component in the β-catenin destruction complex, which provides a scaffold for recruitment of GSK3β, CK1α, and β-catenin, facilitating the phosphorylation and degradation of β-catenin. We therefore examined the effect of ISX9 binding to Axin1 on the interaction of Axin1 and β-catenin. An immunoprecipitation assay was performed in HEK293T cells. As seen in Figure S2, treatment with ISX9 dramatically inhibited the interaction between Axin and β-catenin, but had little effect on the association of β-catenin with GSK3β (Supplementary Figure S2). These results indicated that ISX9 binding to Axin1 could facilitate the release Axin1 from the β-catenin destruction complex.

### 3.6 ISX9 upregulates the expression of Wnt target genes Axin2, LEF1, Fibronectin, and Survivin

Considering that activation of Wnt/β-catenin signaling will upregulate the transcription of Wnt target genes (Mosimann, Hausmann, & Basler, 2009), we assessed the effect of ISX9 on mRNA expression of Wnt target genes Axin2, LEF1, Fibronectin, and Survivin. HEK293T, HaCat and NIH3T3 cells were treated with increasing concentrations of ISX9 (2.5-40 μM) for 24 h. Real-time PCR analysis showed that ISX9 dose-dependently enhanced mRNA expression of Axin2, LEF1, Fibronectin, and Survivin in all three cell lines (Figure 5A-C). Consistent with mRNA data, we detected increased protein levels of Axin2, LEF1, and Survivin in response to ISX9 treatment in all three cell lines (Figure 5D-F). These results confirmed the activation of Wnt/β-catenin signaling in HEK293T, HaCat and NIH3T3 cells treated with ISX9.

### 3.7 ISX9 promotes the expression of stemness marker genes SOX2, LGR5, Twist1, and OCT4

Concerning the importance of the Wnt/β-catenin pathway in the self-renewal and expansion of various stem cell populaces (Ring, Kim, & Kahn, 2014; Tao et al., 2020), the expression of stemness marker genes SOX2, LGR5, Twist1, and OCT4 was examined after treatment with ISX9 by real-time PCR and immunoblotting. As seen in Figure 5, ISX9 treatment significantly enhanced the mRNA of SOX2, LGR5, Twist1, OCT4, and protein levels of SOX2, LGR5, and Twist1 in HEK293T, HaCat and NIH3T3 cells (Figure 5G-L), suggesting that ISX9 may have a potential to promote the stemness property via activating the Wnt/β-catenin pathway.

### 3.8 ISX9 προμοτες ηαιρ ρεγρωτη ιν μιςε ια τικε αςτιατιον οφ Ωντ/β-κιατενιν σικγναλινγ

The Wnt/β-catenin pathway has been shown to play a crucial role in the development of new hair follicles and initiation of hair growth. We next evaluated the effect of ISX9 on the hair regrowth in mice. Minoxidil was exploited as a positive control. ISX9 and minoxidil were topically applied daily to the shaved dorsal skin of 7-week-old C57BL/6 mice. On day 14 and day 21, ISX9 was more effective than minoxidil in promoting hair regrowth in mice. After treatment for 25 days, both ISX9 and minoxidil exhibited strong

hair regrowth-promoting activity compared to control mice (Figure 6A and B). Similar results were obtained by measuring the weight of freshly grown hair (Figure 6C). Histopathology with H&E staining showed significantly increased numbers of hair follicles in the anagen phase on day 25 in ISX9 and minoxidil group compared with that in control mice (Figure 6D), while hair follicles in control mice were still in the telogen phase. Consistently, quantitative analysis of hair follicles also confirmed that the number of hair follicles were markedly increased in ISX9 and minoxidil-treated group compared with control mice (Figure 6E). These results suggest that treatment with ISX9 or minoxidil induces hair follicle transition from telogen to anagen.

We next examined the effect of ISX9 on the Wnt/ $\beta$ -catenin pathway in mice. The results of immunohistochemical staining indicated that ISX9 remarkably increased the expression of active  $\beta$ -catenin, total  $\beta$ -catenin and the Wnt signaling target gene LGR5, concomitant with expression of the proliferation marker Ki-67 (Figure 6F). Moreover, real-time PCR analysis showed that ISX9 treatment significantly upregulated the expression of Wnt target genes (LEF1, Axin2, Fibronectin and Survivin) and stemness marker genes (LGR5, Twist1, SOX2 and OCT4) (Figure 7A and B). Consistent with the above results, ISX9-treated mice exhibited obviously increased protein levels of active  $\beta$ -catenin, total  $\beta$ -catenin, LEF1, Axin2, Survivin, LGR5, and SOX2, while no apparent differences in protein levels of phosphorylated LRP6, total LRP6, CK1 $\epsilon$ , phosphorylated GSK3 $\beta$  and total GSK3 $\beta$  were observed in ISX9, minoxidil and control groups (Figure 7C). Interestingly, we noted that Keratin17 (Waters, Richardson, & Jahoda, 2007), a known-marker of cells with stem cell properties in hair follicle, was also upregulated in response to ISX9 treatment (Figure 7C).

#### 4 DISCUSSION

The Wnt/ $\beta$ -catenin signaling pathway is crucial for neurogenesis (Boitard et al., 2015; McQuate, Latorre-Esteves, & Barria, 2017). The components of Wnt signaling have been involved in neuronal development, neuronal maturation, neuronal differentiation, and proliferation (Varela-Nallar & Inestrosa, 2013). Lie et al reported that the expression of Wnt3 induced neurogenesis in the adult rat dentate gyrus (Lie et al., 2005). The dominant-negative LEF1 could reduce neuronal differentiation induced by co-culture with hippocampal astrocytes (Armenteros, Andreu, Hortigüela, Lie, & Mira, 2018). Wnt7a has been identified as an endogenous regulator of hippocampal neurogenesis that mediates proliferation and neuronal differentiation (Qu et al., 2013). Kuwabara et al found that Wnt/ $\beta$ -catenin signaling could mediate activation of NeuroD1 and play an important role in balancing self-renewal of neural stem cells and neuronal differentiation in adult dentate gyrus (Kuwabara et al., 2009). ISX9 has been identified as a neurogenesis inducer which can upregulate the expression of NeuroD1, promote neurogenesis and enhance neuronal differentiation (Schneider et al., 2008). However, the molecular mechanism underlying ISX9 action in neurogenesis remains unclear. In this study, ISX9 was identified as a potent activator of Wnt/ $\beta$ -catenin signaling. ISX9 could promote the association of LRP6 with Axin1, resulting in the accumulation of  $\beta$ -catenin and the upregulation of Wnt target genes and stemness marker genes. The Wnt agonistic actions of ISX9 may contribute to its functions in neurogenesis.

Axin is a critical scaffolding protein of in the Wnt/ $\beta$ -catenin pathway (Kim et al., 2013). Upon binding of a Wnt ligand to its specific receptor complex, the Wnt co-receptor LRP5/6 is immediately phosphorylated, which generates a docking site for Axin1. Subsequently, the Axin-GSK3 $\beta$  complex is recruited to the receptor, which facilitates GSK3 $\beta$ -induced LRP5/6 phosphorylation and inhibits  $\beta$ -catenin phosphorylation, resulting in the stabilization of  $\beta$ -catenin (Liu et al., 2022). Axin1 has been identified as a cellular target for small molecular compound HLY78. HLY78 could bind to the DIX domain of Axin1 and potentiates the Axin1-LRP6 association, thus activating the Wnt signaling transduction (Wang et al., 2013). Gwak et al reported that the small molecular compound SKL2001 could stabilize intracellular  $\beta$ -catenin via blocking the Axin/ $\beta$ -catenin interaction (Gwak et al., 2012). In our study, ISX9 was found to potently induce the accumulation of intracellular  $\beta$ -catenin without influencing the expression and activity of LRP6 and GSK3 $\beta$ . By covalently binding to the N-terminal region (aa1-300) of Axin1, ISX9 abrogated the association of Axin1 with  $\beta$ -catenin. Meanwhile, ISX9 exhibited a strong promoting effect on the interaction between LRP6 and Axin1, thus leading to stabilizing intracellular  $\beta$ -catenin. Together, our results uncover a novel mechanism by which ISX9 induces the accumulation of  $\beta$ -catenin and activates the Wnt/ $\beta$ -catenin cascade.

The periodic growth of hair follicles includes the three phases of telogen, anagen, and catagen (Lin, Zhu, & He, 2022; Müller-Röver et al., 2001). The cessation of these cyclic phases is the major mechanism contributing to the pathogenesis of alopecia (Petukhova et al., 2010). Accumulating evidence has demonstrated that the hair follicle stem cells are located in the bulge area of the hair follicle and are required for the growth of hair follicles (Liu et al., 2021; Schneider, Schmidt-Ullrich, & Paus, 2009). As a subpopulation of adult stem cells with self-renewal ability, the hair follicle stem cells are able to activate and differentiate into various hair follicle cell types for hair follicle regeneration (Mistriotis & Andreadis, 2013). Increasing evidence showed that hair regeneration and growth heavily depends on the Wnt/ $\beta$ -catenin signaling activation in the hair follicle (Andl et al., 2002). Some Wnt/ $\beta$ -catenin signaling activators have been reported to stimulate hair follicle development. Valproic acid (VPA), a histone deacetylase (HDAC) inhibitor, has been found to accelerate hair cycle and stimulate hair growth. VPA could activate the Wnt/ $\beta$ -catenin signaling pathway by inhibiting GSK3 $\beta$  (Lee et al., 2012). Xing et al demonstrated that baicalin, a natural bioactive flavonoid extracted from *Scutellaria baicalensis* Georgi, could promote the growth of hair follicles via activation of Wnt/ $\beta$ -catenin signaling in mice (Xing et al., 2018). KY19382 is one of the newly synthesized analogues of GSK3 $\beta$  inhibitor indirubin-3'-monoxime. It exhibited hair growth-promoting effect by inactivating GSK3 $\beta$  and blocking the interaction between CXXC-type zinc finger protein 5 (CXXC5) and dishevelled (DVL) (Ryu et al., 2021). Ahmed et al. examined the effect of a tocotrienol-rich formulation (TRF) on hair growth. TRF could reduce the expression of epidermal E-cadherin, and increase nuclear translocation of  $\beta$ -catenin and its interaction with TCF3. Topical application of TRF markedly induced epidermal hair follicle development and early anagen induction (Ahmed et al., 2017). Currently, the drugs for promoting hair growth by targeting Wnt/ $\beta$ -catenin signaling are not yet commercially available. Here, our results revealed that ISX9 could potentially activate Wnt/ $\beta$ -catenin signaling and upregulate the expression of stemness marker genes LEF1, LGR5, Twist1, SOX2, OCT4 and Keratin17. Importantly, ISX9 exerted strong hair growth-promoting activity without causing skin abnormalities in mice. These results indicated that ISX9 may have a great potential to be developed as a hair growth-promoting agent for the treatment of alopecia.

In summary, we identified ISX9 as a novel activator of the Wnt/ $\beta$ -catenin signaling pathway. This compound activated Wnt/ $\beta$ -catenin signaling via elevating the level of intracellular  $\beta$ -catenin. ISX9 was found to target Axin1 through covalently binding to the N-terminal region of Axin1. The binding of ISX9 to Axin1 induced the release of Axin1 from the  $\beta$ -catenin destruction complex, and meanwhile triggered the interaction between Axin1 and LRP6, leading to the stabilization of  $\beta$ -catenin. We further showed that ISX9 could upregulate the expression of Wnt signaling target genes and stemness marker genes. Finally, ISX9 demonstrated potent hair growth-promoting activity in mice, accompanied by the upregulation of the Wnt signaling pathway *in vivo*. These results suggested that ISX9 may be a promising therapeutic agent for alopecia.

## REFERENCES

- Ahmed, N. S., Ghatak, S., El Masry, M. S., Gnyawali, S. C., Roy, S., Amer, M., . . . Khanna, S. (2017). Epidermal E-Cadherin Dependent  $\beta$ -Catenin Pathway Is Phytochemical Inducible and Accelerates Anagen Hair Cycling. *Mol Ther*, *25* (11), 2502-2512. doi:10.1016/j.ymthe.2017.07.010
- Andl, T., Reddy, S. T., Gaddapara, T., & Millar, S. E. (2002). WNT signals are required for the initiation of hair follicle development. *Dev Cell*, *2* (5), 643-653. doi:10.1016/s1534-5807(02)00167-3
- Armenteros, T., Andreu, Z., Hortigüela, R., Lie, D. C., & Mira, H. (2018). BMP and WNT signalling cooperate through LEF1 in the neuronal specification of adult hippocampal neural stem and progenitor cells. *Scientific Reports*, *8* (1), 9241-9241. doi:10.1038/s41598-018-27581-0
- Bettio, L. E. B., Patten, A. R., Gil-Mohapel, J., O'Rourke, N. F., Hanley, R. P., Kennedy, S., . . . Christie, B. R. (2016). ISX-9 can potentiate cell proliferation and neuronal commitment in the rat dentate gyrus. *Neuroscience*, *332*, 212-222. doi:https://doi.org/10.1016/j.neuroscience.2016.06.042
- Boitard, M., Bocchi, R., Egervari, K., Petrenko, V., Viale, B., Gremaud, S., . . . Kiss, Jozsef Z. (2015). Wnt Signaling Regulates Multipolar-to-Bipolar Transition of Migrating Neurons in the Cerebral Cortex. *Cell Reports*, *10* (8), 1349-1361. doi:https://doi.org/10.1016/j.celrep.2015.01.061

- Bolduc, C., & Shapiro, J. (2000). Management of androgenetic alopecia. *Am J Clin Dermatol*, *1* (3), 151-158. doi:10.2165/00128071-200001030-00002
- Chai, M., Jiang, M., Vergnes, L., Fu, X., de Barros, S. C., Doan, N. B., . . . Huang, J. (2019). Stimulation of Hair Growth by Small Molecules that Activate Autophagy. *Cell Rep*, *27* (12), 3413-3421.e3413. doi:10.1016/j.celrep.2019.05.070
- Clevers, H., & Nusse, R. (2012). Wnt/ $\beta$ -catenin signaling and disease. *Cell*, *149* (6), 1192-1205. doi:10.1016/j.cell.2012.05.012
- Curtis, M. J., Alexander, S., Cirino, G., Docherty, J. R., George, C. H., Giembycz, M. A., . . . Ahluwalia, A. (2018). Experimental design and analysis and their reporting II: updated and simplified guidance for authors and peer reviewers. *British journal of pharmacology*, *175* (7), 987-993. doi:10.1111/bph.14153
- Dioum, E. M., Osborne, J. K., Goetsch, S., Russell, J., Schneider, J. W., & Cobb, M. H. (2011). A small molecule differentiation inducer increases insulin production by pancreatic  $\beta$  cells. *Proc Natl Acad Sci U S A*, *108* (51), 20713-20718. doi:10.1073/pnas.1118526109
- Dong, L., Hao, H., Xia, L., Liu, J., Ti, D., Tong, C., . . . Han, W. (2014). Treatment of MSCs with Wnt1a-conditioned medium activates DP cells and promotes hair follicle regrowth. *Scientific Reports*, *4* (1), 5432. doi:10.1038/srep05432
- Gwak, J., Hwang, S. G., Park, H.-S., Choi, S. R., Park, S.-H., Kim, H., . . . Oh, S. (2012). Small molecule-based disruption of the Axin/ $\beta$ -catenin protein complex regulates mesenchymal stem cell differentiation. *Cell Research*, *22* (1), 237-247. doi:10.1038/cr.2011.127
- Hu, X. M., Li, Z. X., Zhang, D. Y., Yang, Y. C., Fu, S. A., Zhang, Z. Q., . . . Xiong, K. (2021). A systematic summary of survival and death signalling during the life of hair follicle stem cells. *Stem Cell Res Ther*, *12* (1), 453. doi:10.1186/s13287-021-02527-y
- Jang, W. S., Son, I. P., Yeo, I. K., Park, K. Y., Li, K., Kim, B. J., . . . Hong, C. K. (2013). The annual changes of clinical manifestation of androgenetic alopecia clinic in korean males and females: a outpatient-based study. *Ann Dermatol*, *25* (2), 181-188. doi:10.5021/ad.2013.25.2.181
- Kalwat, M. A., Huang, Z., Wichaidit, C., McGlynn, K., Earnest, S., Savoia, C., . . . Cobb, M. H. (2016). Isoxazole Alters Metabolites and Gene Expression, Decreasing Proliferation and Promoting a Neuroendocrine Phenotype in  $\beta$ -Cells. *ACS Chem Biol*, *11* (4), 1128-1136. doi:10.1021/acscchembio.5b00993
- Kim, S. E., Huang, H., Zhao, M., Zhang, X., Zhang, A., Semonov, M. V., . . . He, X. (2013). Wnt stabilization of  $\beta$ -catenin reveals principles for morphogen receptor-scaffold assemblies. *Science*, *340* (6134), 867-870. doi:10.1126/science.1232389
- Koh, S. H., Liang, A. C., Takahashi, Y., Maki, T., Shindo, A., Osumi, N., . . . Lo, E. H. (2015). Differential Effects of Isoxazole-9 on Neural Stem/Progenitor Cells, Oligodendrocyte Precursor Cells, and Endothelial Progenitor Cells. *PLoS One*, *10* (9), e0138724. doi:10.1371/journal.pone.0138724
- Kratochwil, K., Dull, M., Farinas, I., Galceran, J., & Grosschedl, R. (1996). Lef1 expression is activated by BMP-4 and regulates inductive tissue interactions in tooth and hair development. *Genes Dev*, *10* (11), 1382-1394. doi:10.1101/gad.10.11.1382
- Kuwabara, T., Hsieh, J., Muotri, A., Yeo, G., Warashina, M., Lie, D. C., . . . Gage, F. H. (2009). Wnt-mediated activation of NeuroD1 and retro-elements during adult neurogenesis. *Nature neuroscience*, *12* (9), 1097-1105. doi:10.1038/nn.2360
- Kwack, M. H., Kim, M. K., Kim, J. C., & Sung, Y. K. (2012). Dickkopf 1 promotes regression of hair follicles. *J Invest Dermatol*, *132* (6), 1554-1560. doi:10.1038/jid.2012.24
- Lee, S. H., Yoon, J., Shin, S. H., Zahoor, M., Kim, H. J., Park, P. J., . . . Choi, K. Y. (2012). Valproic acid induces hair regeneration in murine model and activates alkaline phosphatase activity in human dermal

papilla cells. *PLoS One*, 7 (4), e34152. doi:10.1371/journal.pone.0034152

Libecco, J. F., & Bergfeld, W. F. (2004). Finasteride in the treatment of alopecia. *Expert Opin Pharmacother*, 5 (4), 933-940. doi:10.1517/14656566.5.4.933

Lie, D. C., Colamarino, S. A., Song, H. J., Désiré, L., Mira, H., Consiglio, A., . . . Gage, F. H. (2005). Wnt signalling regulates adult hippocampal neurogenesis. *Nature*, 437 (7063), 1370-1375. doi:10.1038/nature04108

Lilley, E., Stanford, S. C., Kendall, D. E., Alexander, S. P. H., Cirino, G., Docherty, J. R., . . . Ahluwalia, A. (2020). ARRIVE 2.0 and the British Journal of Pharmacology: Updated guidance for 2020. *177* (16), 3611-3616. doi:<https://doi.org/10.1111/bph.15178>

Lin, X., Zhu, L., & He, J. (2022). Morphogenesis, Growth Cycle and Molecular Regulation of Hair Follicles. *10* . doi:10.3389/fcell.2022.899095

Linas, S. L., & Nies, A. S. (1981). Minoxidil. *Ann Intern Med*, 94 (1), 61-65. doi:10.7326/0003-4819-94-1-61

Liu, F., Zhang, X., Peng, Y., Zhang, L., Yu, Y., Hua, P., . . . Zhang, L. (2021). miR-24 controls the regenerative competence of hair follicle progenitors by targeting Plk3. *Cell Reports*, 35 (10), 109225. doi:<https://doi.org/10.1016/j.celrep.2021.109225>

Liu, J., Xiao, Q., Xiao, J., Niu, C., Li, Y., Zhang, X., . . . Yin, G. (2022). Wnt/ $\beta$ -catenin signalling: function, biological mechanisms, and therapeutic opportunities. *Signal Transduction and Targeted Therapy*, 7 (1), 3. doi:10.1038/s41392-021-00762-6

McQuate, A., Latorre-Esteves, E., & Barria, A. (2017). A Wnt/Calcium Signaling Cascade Regulates Neuronal Excitability and Trafficking of NMDARs. *Cell Rep*, 21 (1), 60-69. doi:10.1016/j.celrep.2017.09.023

Mistriotis, P., & Andreadis, S. T. (2013). Hair follicle: a novel source of multipotent stem cells for tissue engineering and regenerative medicine. *Tissue Eng Part B Rev*, 19 (4), 265-278. doi:10.1089/ten.TEB.2012.0422

Mosimann, C., Hausmann, G., & Basler, K. (2009). Beta-catenin hits chromatin: regulation of Wnt target gene activation. *Nat Rev Mol Cell Biol*, 10 (4), 276-286. doi:10.1038/nrm2654

Müller-Röver, S., Handjiski, B., van der Veen, C., Eichmüller, S., Foitzik, K., McKay, I. A., . . . Paus, R. (2001). A comprehensive guide for the accurate classification of murine hair follicles in distinct hair cycle stages. *J Invest Dermatol*, 117 (1), 3-15. doi:10.1046/j.0022-202x.2001.01377.x

Noramly, S., Freeman, A., & Morgan, B. A. (1999). beta-catenin signaling can initiate feather bud development. *Development*, 126 (16), 3509-3521. doi:10.1242/dev.126.16.3509

Nusse, R., & Clevers, H. (2017). Wnt/ $\beta$ -Catenin Signaling, Disease, and Emerging Therapeutic Modalities. *Cell*, 169 (6), 985-999. doi:10.1016/j.cell.2017.05.016

Ouji, Y., Yoshikawa, M., Moriya, K., Nishiofuku, M., Matsuda, R., & Ishizaka, S. (2008). Wnt-10b, uniquely among Wnts, promotes epithelial differentiation and shaft growth. *Biochem Biophys Res Commun*, 367 (2), 299-304. doi:10.1016/j.bbrc.2007.12.091

Patel, M., Harrison, S., & Sinclair, R. (2013). Drugs and hair loss. *Dermatol Clin*, 31 (1), 67-73. doi:10.1016/j.det.2012.08.002

Petukhova, L., Duvic, M., Hordinsky, M., Norris, D., Price, V., Shimomura, Y., . . . Christiano, A. M. (2010). Genome-wide association study in alopecia areata implicates both innate and adaptive immunity. *Nature*, 466 (7302), 113-117. doi:10.1038/nature09114

Pratt, C. H., King, L. E., Jr., Messenger, A. G., Christiano, A. M., & Sundberg, J. P. (2017). Alopecia areata. *Nat Rev Dis Primers*, 3 , 17011. doi:10.1038/nrdp.2017.11

Qu, Q., Sun, G., Murai, K., Ye, P., Li, W., Asuelime, G., . . . Shi, Y. (2013). Wnt7a regulates multiple steps of neurogenesis. *Mol Cell Biol*, 33 (13), 2551-2559. doi:10.1128/mcb.00325-13

- Rajendran, R. L., Gangadaran, P., Seo, C. H., Kwack, M. H., Oh, J. M., Lee, H. W., . . . Ahn, B. C. (2020). Macrophage-Derived Extracellular Vesicle Promotes Hair Growth. *Cells*, *9* (4). doi:10.3390/cells9040856
- Ring, A., Kim, Y.-M., & Kahn, M. (2014). Wnt/catenin signaling in adult stem cell physiology and disease. *Stem cell reviews and reports*, *10* (4), 512-525. doi:10.1007/s12015-014-9515-2
- Ryu, Y. C., Lee, D.-H., Shim, J., Park, J., Kim, Y.-R., Choi, S., . . . Choi, K.-Y. (2021). KY19382, a novel activator of Wnt/ $\beta$ -catenin signalling, promotes hair regrowth and hair follicle neogenesis. *British journal of pharmacology*, *178* (12), 2533-2546. doi:10.1111/bph.15438
- Schneider, J. W., Gao, Z., Li, S., Farooqi, M., Tang, T. S., Bezprozvanny, I., . . . Hsieh, J. (2008). Small-molecule activation of neuronal cell fate. *Nat Chem Biol*, *4* (7), 408-410. doi:10.1038/nchembio.95
- Schneider, M. R., Schmidt-Ullrich, R., & Paus, R. (2009). The hair follicle as a dynamic miniorgan. *Curr Biol*, *19* (3), R132-142. doi:10.1016/j.cub.2008.12.005
- Sica, D. A. (2004). Minoxidil: an underused vasodilator for resistant or severe hypertension. *J Clin Hypertens (Greenwich)*, *6* (5), 283-287. doi:10.1111/j.1524-6175.2004.03585.x
- Stenn, K. S., & Paus, R. (2001). Controls of hair follicle cycling. *Physiol Rev*, *81* (1), 449-494. doi:10.1152/physrev.2001.81.1.449
- Tamai, K., Semenov, M., Kato, Y., Spokony, R., Liu, C., Katsuyama, Y., . . . He, X. (2000). LDL-receptor-related proteins in Wnt signal transduction. *Nature*, *407* (6803), 530-535. doi:10.1038/35035117
- Tao, F., Soffers, J., Hu, D., Chen, S., Gao, X., Zhang, Y., . . . Li, L. (2020).  $\beta$ -Catenin and Associated Proteins Regulate Lineage Differentiation in Ground State Mouse Embryonic Stem Cells. *Stem Cell Reports*, *15* (3), 662-676. doi:10.1016/j.stemcr.2020.07.018
- Tsakmaki, A., Fonseca Pedro, P., Pavlidis, P., Hayee, B., & Bewick, G. A. (2020). ISX-9 manipulates endocrine progenitor fate revealing conserved intestinal lineages in mouse and human organoids. *Mol Metab*, *34*, 157-173. doi:10.1016/j.molmet.2020.01.012
- Van Neste, D., Fuh, V., Sanchez-Pedreno, P., Lopez-Bran, E., Wolff, H., Whiting, D., . . . Kaufman, K. D. (2000). Finasteride increases anagen hair in men with androgenetic alopecia. *Br J Dermatol*, *143* (4), 804-810. doi:10.1046/j.1365-2133.2000.03780.x
- Varela-Nallar, L., & Inestrosa, N. (2013). Wnt signaling in the regulation of adult hippocampal neurogenesis. *7*. doi:10.3389/fncel.2013.00100
- Wang, S., Yin, J., Chen, D., Nie, F., Song, X., Fei, C., . . . Li, L. (2013). Small-molecule modulation of Wnt signaling via modulating the Axin-LRP5/6 interaction. *Nat Chem Biol*, *9* (9), 579-585. doi:10.1038/nchembio.1309
- Waters, J. M., Richardson, G. D., & Jahoda, C. A. (2007). Hair follicle stem cells. *Semin Cell Dev Biol*, *18* (2), 245-254. doi:10.1016/j.semcdb.2007.02.003
- Wu, Z., Zhu, Y., Liu, H., Liu, G., & Li, F. (2020). Wnt10b promotes hair follicles growth and dermal papilla cells proliferation via Wnt/ $\beta$ -Catenin signaling pathway in Rex rabbits. *Bioscience Reports*, *40* (2). doi:10.1042/bsr20191248
- Xing, F., Yi, W. J., Miao, F., Su, M. Y., & Lei, T. C. (2018). Baicalin increases hair follicle development by increasing canonical Wnt/ $\beta$ -catenin signaling and activating dermal papillar cells in mice. *Int J Mol Med*, *41* (4), 2079-2085. doi:10.3892/ijmm.2018.3391
- Xuan, W., Wang, Y., Tang, Y., Ali, A., Hu, H., Maienschein-Cline, M., & Ashraf, M. (2018). Cardiac Progenitors Induced from Human Induced Pluripotent Stem Cells with Cardiogenic Small Molecule Effectively Regenerate Infarcted Hearts and Attenuate Fibrosis. *Shock*, *50* (6), 627-639. doi:10.1097/shk.0000000000001133



405 nm). (F) MS spectra of protein-ligand complex formed between Axin1-300 and ISX9. The blue arrow indicated molecular weight of protein, red arrow indicated molecular weight of the protein-ligand complex. The molecular weight of ligand ISX9 was calculated as 233.44.

**Figure 5. ISX9 upregulates the expression of Wnt target genes and stemness marker genes.** HEK293T (A), HaCat (B), and NIH3T3 (C) cells were incubated with vehicle control (DMSO) or the indicated concentrations of ISX9 (2.5-40  $\mu$ M) for 24 h. Total RNA was extracted and cDNAs were obtained by reverse transcription, and then subjected to real-time PCR analysis to detect the mRNA expression of Axin2, LEF1, Fibronectin and Survivin. The results were shown as mean  $\pm$  SD from three independent experiments. HEK293T (D), HaCat (E), and NIH3T3 (F) cells were treated with vehicle control (DMSO) or the indicated concentrations of ISX9 (2.5-40  $\mu$ M) for 24 h. Protein expression of Axin2, LEF1 and Survivin were detected by immunoblotting. Data shown were representative of three independent experiments. The relative expression levels of Axin2, LEF1, Fibronectin and Survivin, were quantified after normalization to GAPDH. \* $p < 0.05$ , compared to vehicle control. HEK293T (G), HaCat (H) and NIH3T3 (I) cells were incubated with vehicle control (DMSO) or the indicated amounts of ISX9 (2.5-40  $\mu$ M) for 24 h. Total RNA was extracted and then reverse-transcribed into cDNA. Prepared cDNAs were subjected to quantitative PCR analysis to detect the mRNA expression of stemness marker genes SOX2, LGR5, Twist1, and OCT4. The protein levels of stemness marker genes SOX2, LGR5, and Twist1 were measured with immunoblotting after treatment with the indicated doses of ISX9 in HEK293T (J), HaCat (K) and NIH3T3 cells (L) respectively. Data shown were representative of three independent experiments. The relative expression levels of SOX2, LGR5, Twist1, and OCT4 were quantified after normalization to GAPDH. \* $p < 0.05$ , compared to vehicle control.

**Figure 6. ISX9 promotes hair regrowth *in vivo*.** C57BL/6J mice in the telogen phase (7 weeks old) were depilated. Vehicle (50% [v/v] ethanol, 30% water and 20% propylene glycol), 1% ISX9, or 2% minoxidil were topically applied daily to the dorsal skin for 25 days (n = 5 per group) (A) Representative photos of mice showed hair regrowth on mentioned days treated with each drug. (B) Quantitative measurements of hair coat recovery at the designated area from 0-25 days. (C) Gross analyses of weight of regrown hair in different groups treated for 25 days. (D) Haematoxylin and eosin (H&E) staining to assess the hair follicles of skins in different groups treated (vertical and transverse view) (E) Quantitative evaluation of the comparative number of hair follicles of HE staining images (n = 5) (F) Immunohistochemistry (IHC) staining for active and total  $\beta$ -catenin, Ki67 and LGR5 using the dorsal skin of mice treated with each drug for 25 days. Scale bars = 50  $\mu$ m. Values are expressed as means  $\pm$  SEM. \* $p < 0.05$  and \*\* $p < 0.01$ , significantly different, ns, not significant.

**Figure 7. ISX9 promotes the expression of hair regrowth-related markers in C57BL/6J mice.** The vehicle control, 1% ISX9, or 2% minoxidil were topically applied daily to the dorsal skin for 25 days after depilation. (n = 5 per group). (A) The expression of the indicated genes, LEF1, Axin2, Fibronectin, and Survivin in each treated mouse was quantified by real-time PCR analysis on day 25. (B) The expression of the indicated gene, LGR5, Twist1, SOX2 and OCT4 in each treatment group was measured using real-time PCR analysis on day 25. (C) Immunoblotting analyses for phosphorylated LRP6, total LRP6, CK1 $\epsilon$ , phosphorylated GSK3 $\beta$ , total GSK3 $\beta$ , active  $\beta$ -catenin, total  $\beta$ -catenin, LEF1, Axin2, Survivin, LGR5, SOX2, and Keratin17 on day 25. Values are expressed as means  $\pm$  SEM. \* $p < 0.05$  and \*\* $p < 0.01$ , significantly different; ns, not significant.

## SUPPLEMENTAL FIGURES

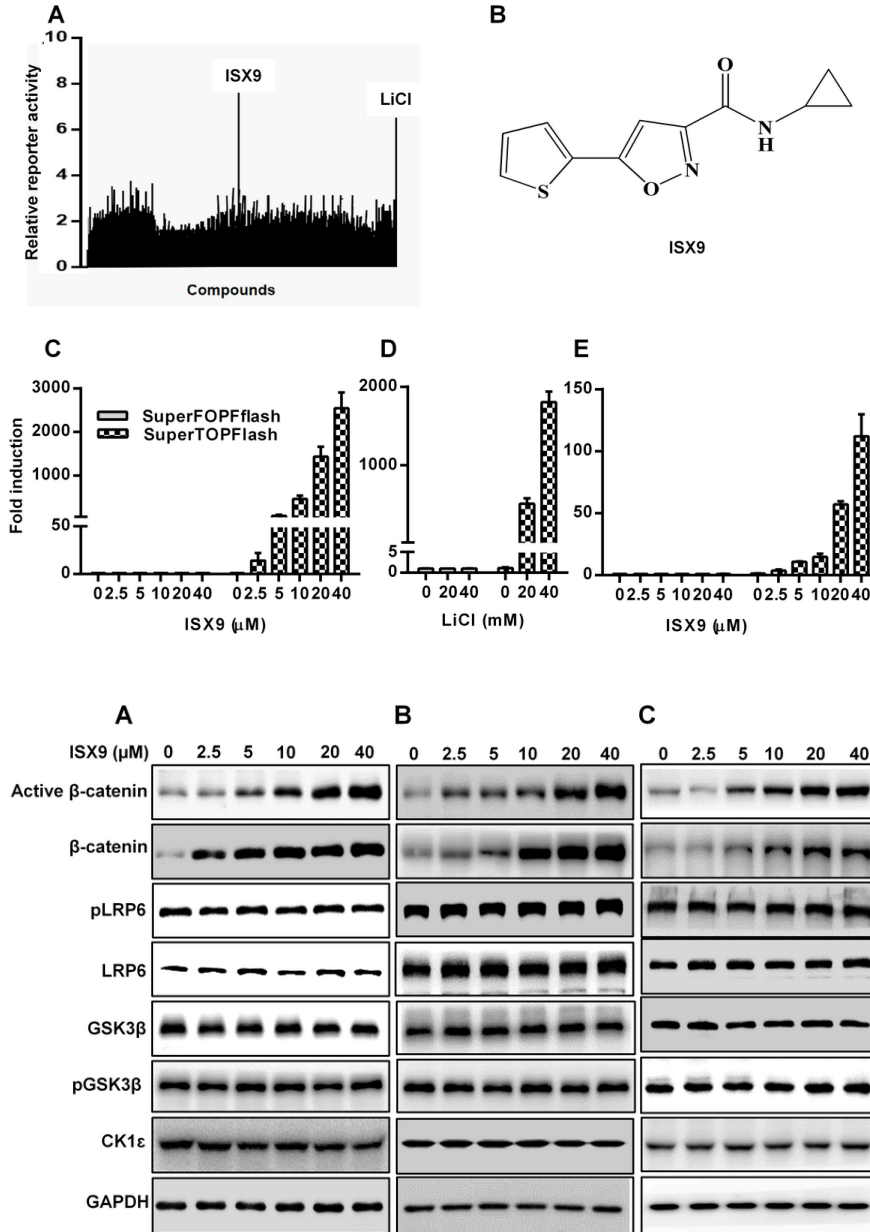
**Φιγυρε Σ1. Τρεατμεντ ωιτη ΙΣΧ9 δοες νοτ αφφερετ τηε μΡΝΑ εξπρεσσιον οφ β-κατενιν ιν ΗΕΚ293Τ ανδ ΗαCατ ρελλετς.** (A) HEK293T and (B) HaCat cells were treated with the indicated concentrations of ISX9 for 24 h. The relative mRNA level of  $\beta$ -catenin was measured by real-time PCR. The data from three independent experiments are presented.

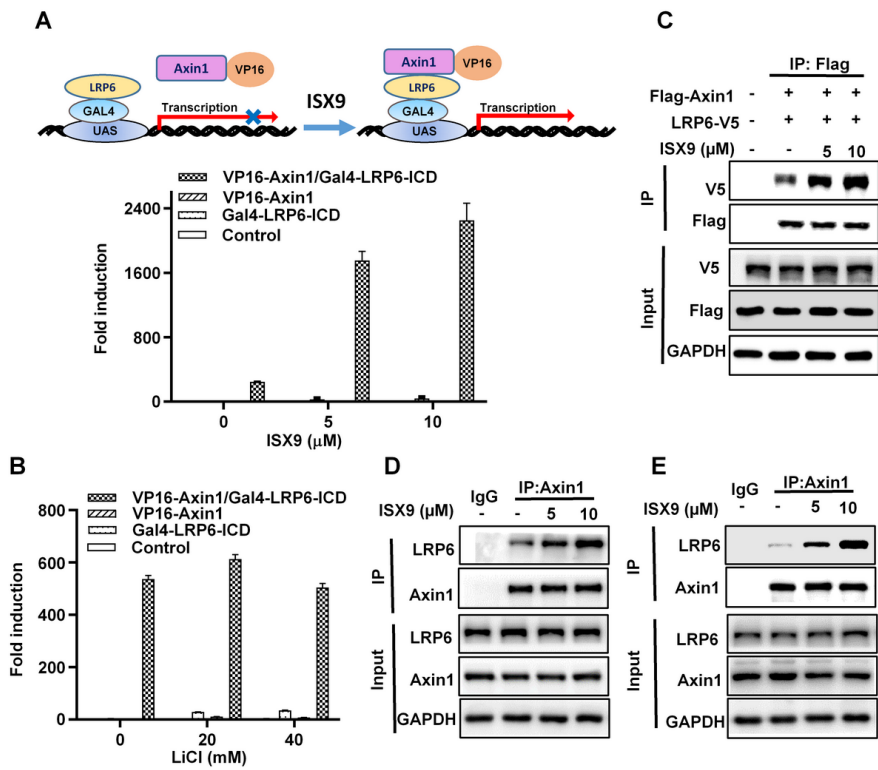
**Φιγυρε Σ2. ΙΣΧ9 ινηιβιτετ τηε ιντερακτιον οφ Αξιn1 ωιτη β-κατενιν.** HEK293T cells were incubated with the indicated concentrations of ISX9 for 24 h. Cell lysates were extracted and subjected to im-

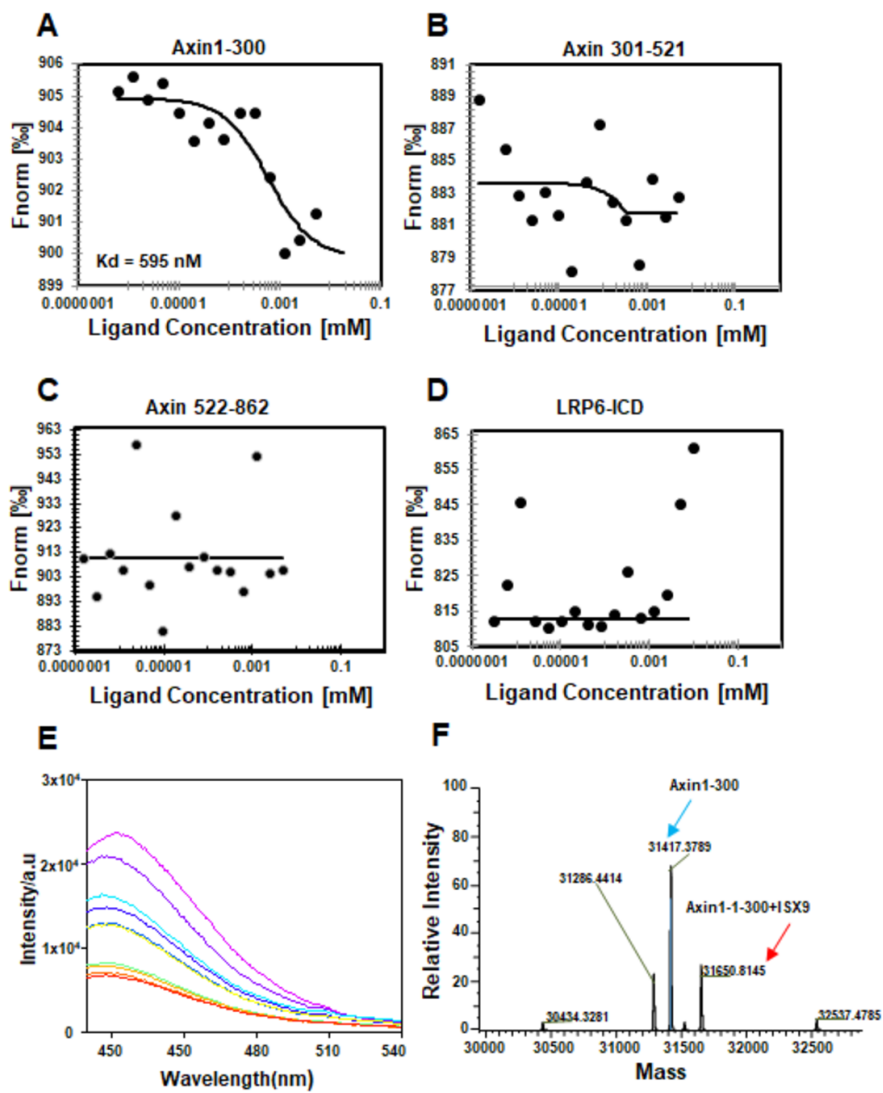
munoprecipitation (IP) using anti- $\beta$ -catenin antibody followed by Western blotting using specific antibodies as indicated.

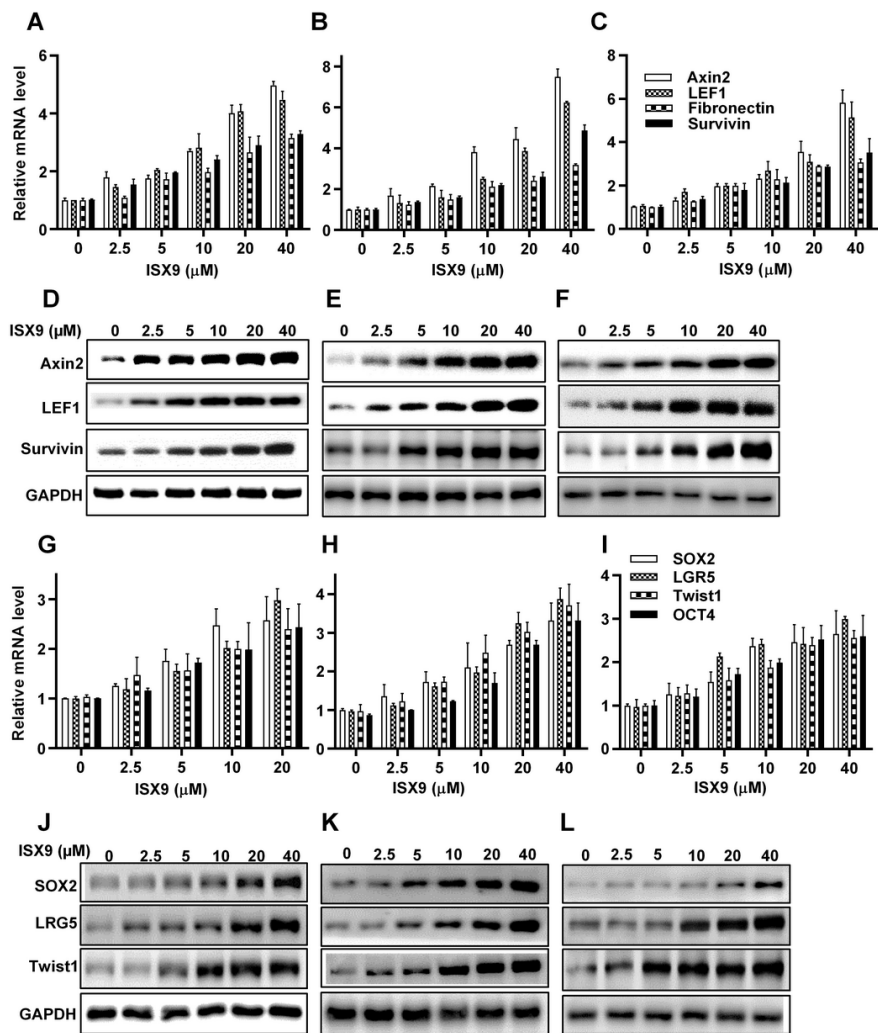
## SUPPLEMENTARY INFORMATION

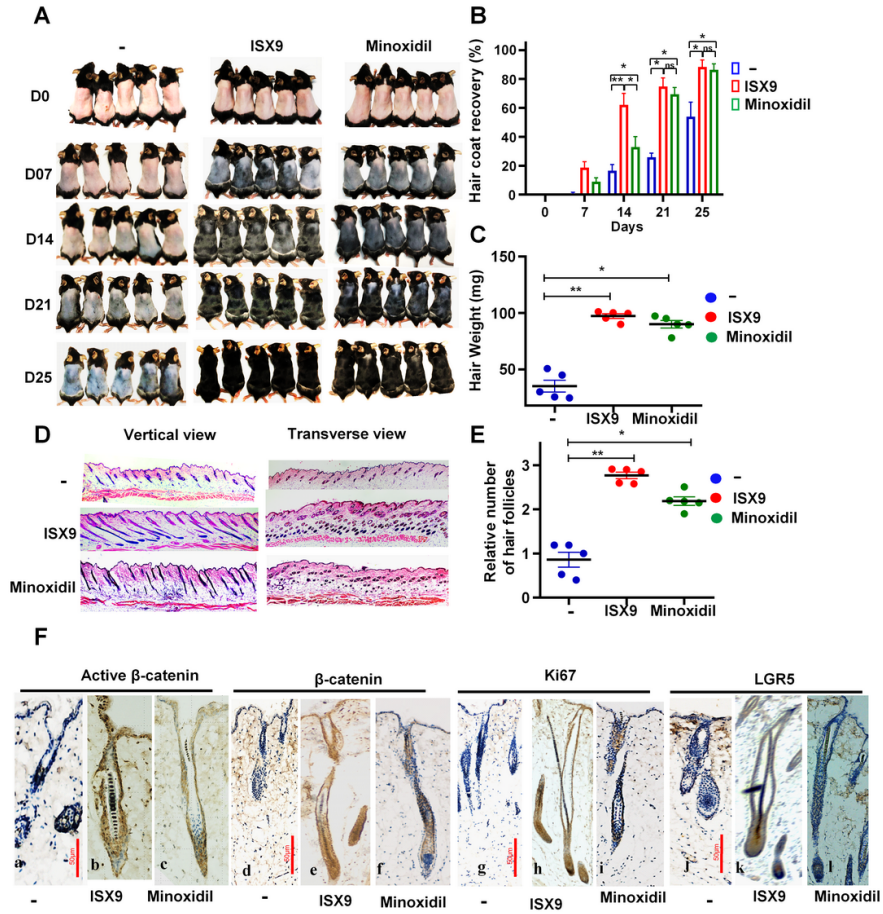
Supplementary Information includes two figures and 2 tables

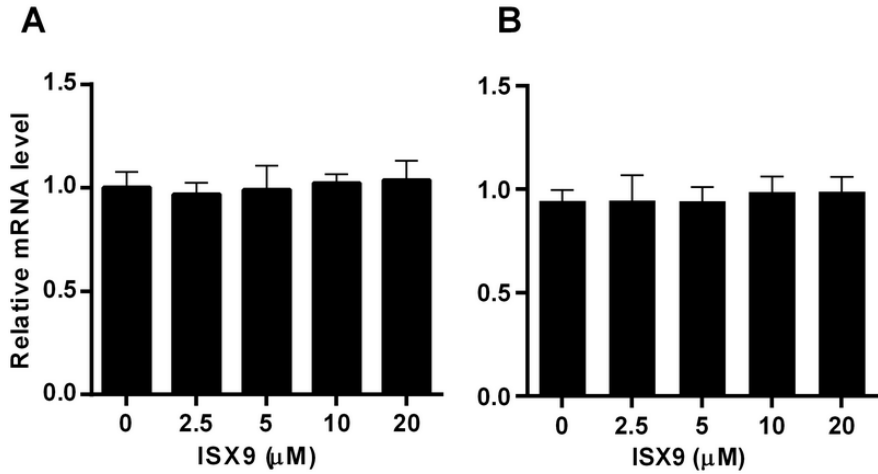
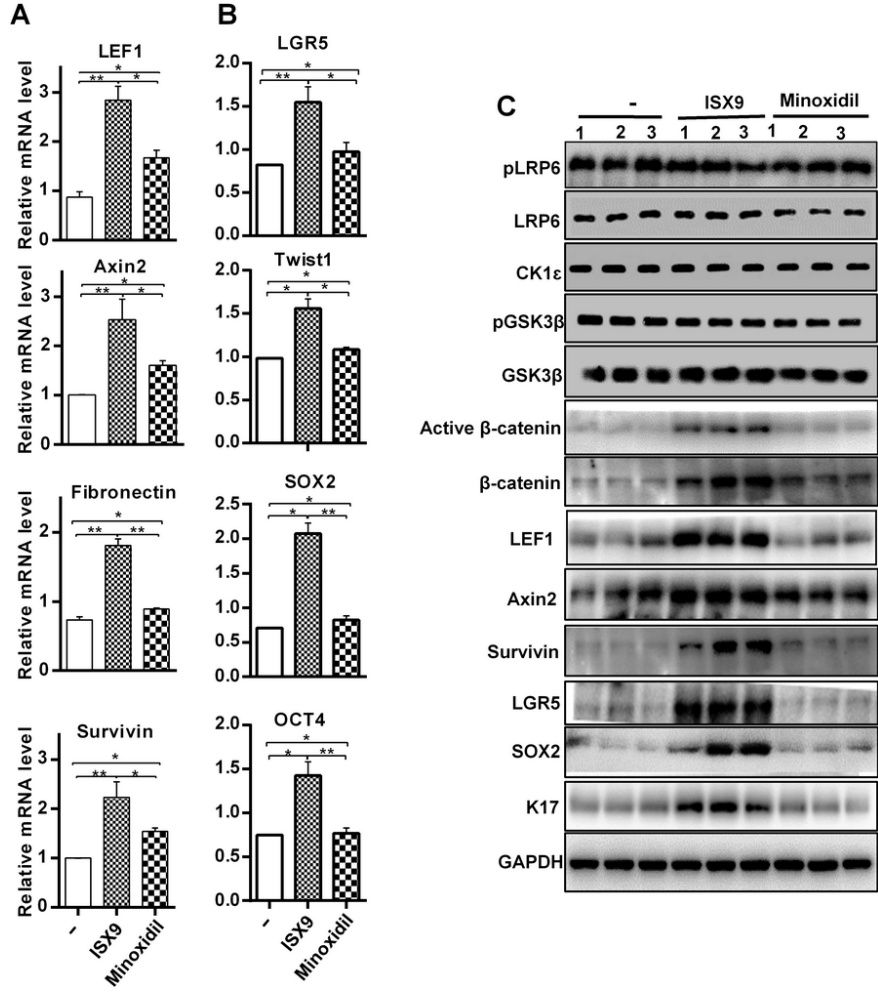


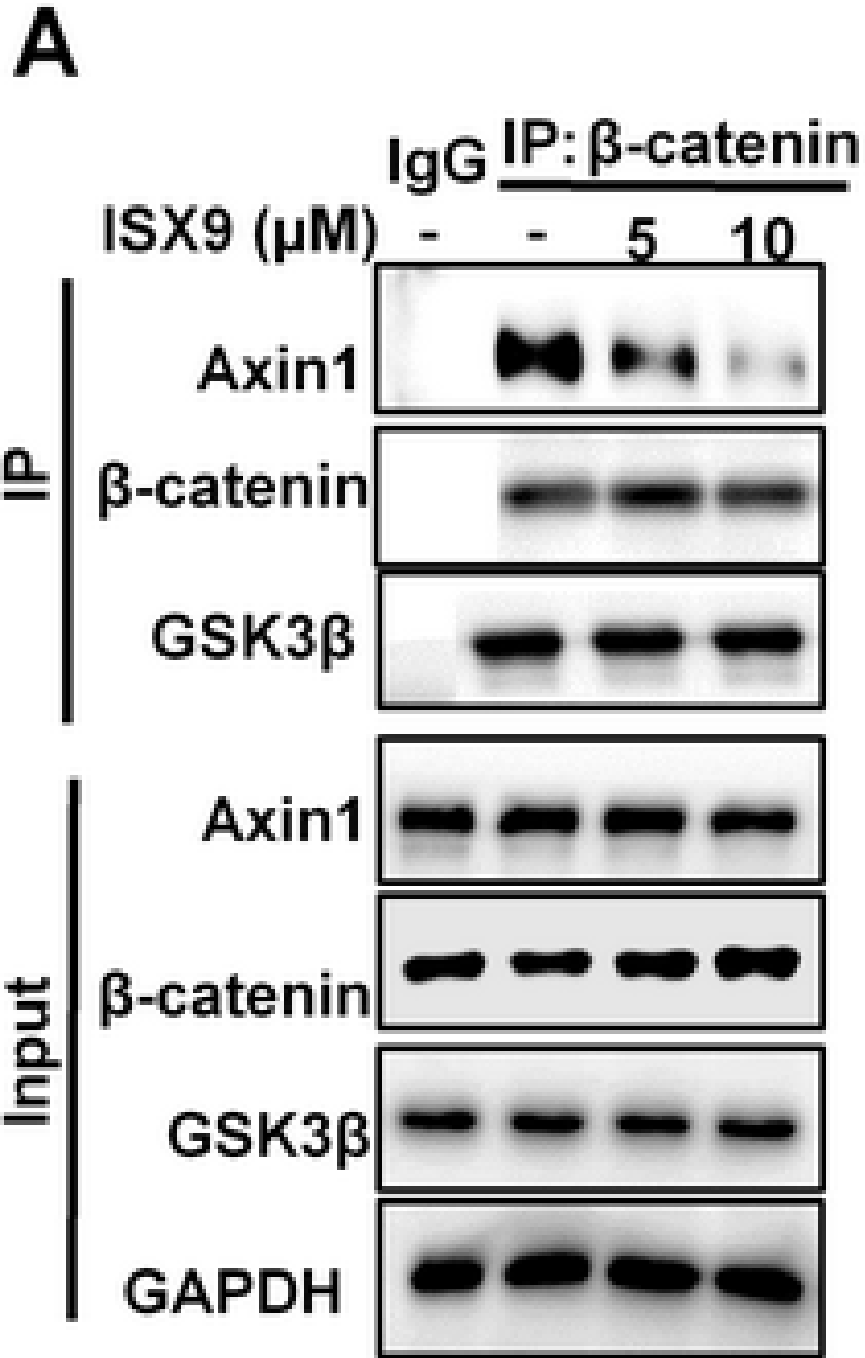












Hosted file

Supplementary table-.docx available at <https://authorea.com/users/503180/articles/582965-isx9-a-small-molecule-targeting-axin-activates-wnt-%CE%B2-catenin-signaling-and-promotes-hair-regrowth>